Turkish Journal of Electrical Engineering & Computer Sciences

http://journals.tubitak.gov.tr/elektrik/

Research Article

Turk J Elec Eng & Comp Sci
(2015) 23: 1272 – 1283

doi:10.3906/elk-1303-72

A new approach to the development of a nonlinear model for micro-Pelton turbines

Mahmut Temel ÖZDEMİR*, Ahmet ORHAN
Department of Electrical and Electronics Engineering, Faculty of Engineering, Fırat University, Elazığ, Turkey

Received: 12.03.2013 • **Accepted/Published Online:** 26.06.2013 • **Printed:** 28.08.2015

Abstract: In this study, a new approach that is closer to the real turbine without abandoning the advantages of nonlinear modeling simplicity compromising the simplicity of the nonlinear model is proposed. The purpose of the study is to contribute to making theoretical studies of microhydroelectric power plants (MHPPs) more realistic. Studies on their control, especially frequency control, have increased with the expansion of grid-connected power plants. However, some problems have occurred when converting simulation studies of the frequency control to practical studies. The reasons for these problems are that the systems cannot be modeled completely. In this study, first, the nonlinear model equations of a Pelton turbine are primarily constituted. The efficiency curve of the turbine is then obtained experimentally and added to the nonlinear model. The simulation results are compared with the data obtained from the prototype MHPP with a Pelton turbine developed in the laboratory. Finally, it is seen that the proposed method is successful. Thus, with the help of the proposed method, theoretical studies that researchers do can be easily converted into practical applications.

Key words: Nonlinear hydraulic turbine model, micro-Pelton turbine, microhydro power plant

1. Introduction

Hydroelectric power plants (HPPs) are widely used and well-known energy production units all around the world. HPPs meet approximately 20% of the total electricity need of the world [1]. Generally, large power plants are preferred for electricity generation around the world, except for in a few countries. Therefore, it is not very common to produce electricity using small and microscale HPPs. This situation offers significant opportunities for small-scale and very-small-scale businesses.

The modeling of microhydroelectric power plants (MHPPs) is the basis of many theoretical and practical research studies. The general structures of large-scale HPPs and MHPPs are basically the same. Therefore, previous studies employed models of large-scale HPPs in the modeling of MHPPs [2–13].

The general model of the speed controller of a HPP is shown in Figure 1. It is evident from the model that the more realistic the hydraulic turbine model is that is used to actuate the generator, the more realistic the simulation results will become.

The MHPP has a prominent advantage compared to large- and very-large-scale HPPs in terms of its power specifications. In this respect, this study turns the small physical size of the MHPP into an advantage and points out an overlooked aspect.

*Correspondence: mto@firat.edu.tr

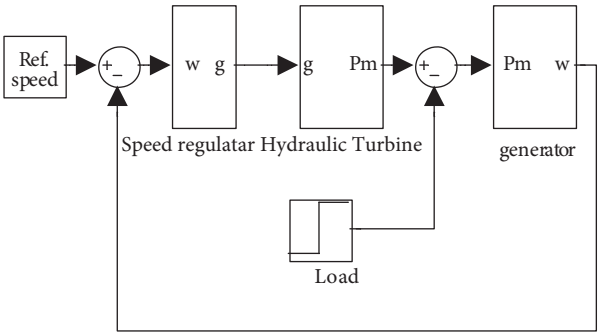

Figure 1. Speed control loop.

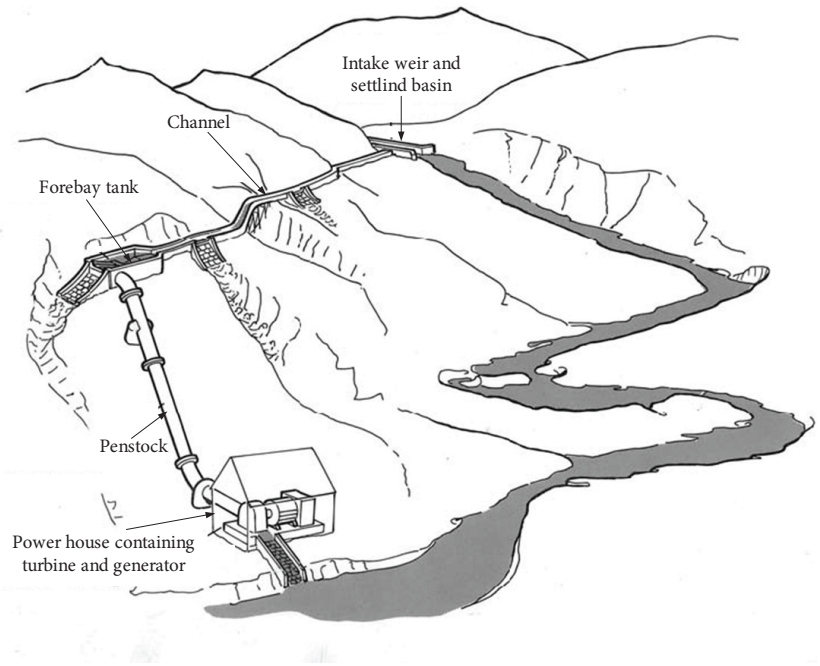

Figure 2. Schematic view of a conventional MHPP.

A conventional MHPP model is shown in Figure 2. There is no water collection process in the MHPPs mostly built as river-type power plants. Instead, there exists a structure (forebay) at the penstock and river connection point that regulates the water height. Therefore, MHPPs do not cause the negative environmental impacts (such as inundation of residential and historical areas, deterioration of ecological structures, etc.) that are often caused by the large-scale HPPs [14]. Although there are different classifications of HPPs, the most accepted one is the classification of UNIDO. According to this classification, MHPPs have installed power ranging between 5 and 100 kW [15].

In practical applications of MHPPs, either some parts are not used or the functions of these parts are fulfilled by other components under certain assumptions [4,5,9,16–19]. These assumptions help prevent most of the problems beforehand. However, the system becomes more unrealistic due to the fact that although the equipment, machine, or situation is tried to be made more realistic, it cannot be ignored that there are some major deficiencies in the system and therefore it cannot represent the real system.

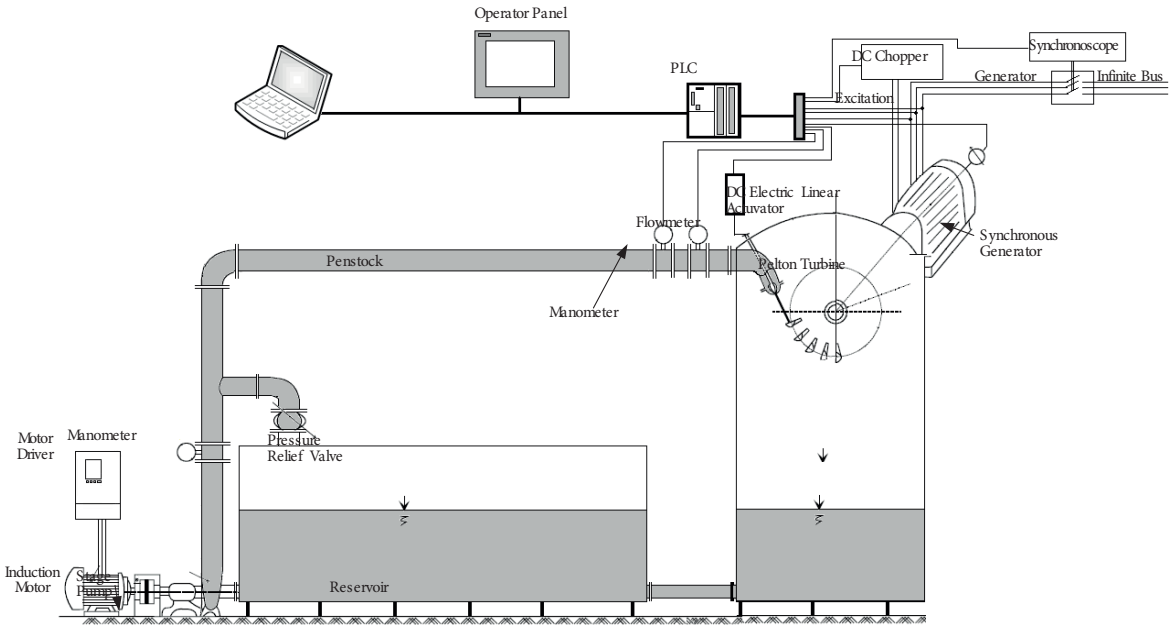

Figure 3. Schematic view of prototype MHPP.

The prototype MHPP used in this study is developed such that it can work in the laboratory environment. The general figure of the prototype is given in Figure 3. All possible situations that can occur in a conventional MHPP were modeled with the help of this prototype. Testing of different turbines or of experiments on the same turbine under different operating conditions can be carried out with this prototype.

Speed-frequency control of the HPP changes depending on local or parallel operation. In local operation, this control is achieved by two basic methods. The first method employs the flow rate setting change. In this method, as the turbine speed changes, the amount of water transferred to the turbine is changed inversely proportional to the turbine speed change. Flow rate is increased when the turbine speed is decreased and vice versa. The other method is the load control method. In this method, the flow rate is not changed. The control is achieved by switching of the backup load connected to the generator.

The prototype was designed to employ both of the control methods mentioned above. The flow rate setting method was used in the experimental studies. The prototype works as follows: The pressure of the water taken from a 1-t water tank is set to the desired pressure value with the help of a multistage pump, after which it is directed to the penstock. The water in the penstock has high pressure and low speed. This water hits the blades of the Pelton turbine, the turbine rotates the synchronous generator, and the water is sent back to the water tank. The voltage of the generator is controlled by an excitation current source and its related circuitry. The frequency of the generator, i.e. the speed of the turbine, is controlled by a linear electrical activator and its driver. A programmable logic controller (PLC) is used to control and command the whole system.

Recently, the use of novel control techniques in MHPPs employing voltage and especially frequency control has made it possible for the MHPP to become widespread. However, many problems are encountered when the simulation studies of frequency control are put into practice. The reason for these problems is that the system is not modeled accurately. Many different hydraulic turbine models are used in the simulation of HPPs. These models are basically categorized into two groups, as linear and nonlinear models. In this study, a high-fidelity modeling approach is proposed without compromising the simplicity of the linear model. The efficiency curve

of the turbine is obtained by experiments and added to the model. The simulation results are compared to the data obtained from the prototype MHPP with a Pelton turbine in the laboratory environment. Experimental results are obtained at different needle aperture and pressure values. The success of the proposed methodology is presented and discussed in the conclusion.

2. Materials and methods

Modeling of a HPP is achieved in two phases taking into account the hydraulic, mechanical, and electrical conversions. These are the turbine-speed regulator model and the generator model. The turbine is the most important and characteristic component in the turbine-speed regulator model. Many different turbine models are used for the modeling of hydraulic turbines. In the literature, several models allowing for a comprehensive investigation of fluid mechanics have been studied and developed, such as linear and nonlinear models, nonlinear models with progressive wave theory, and nonlinear models with progressive wave theory and surge tank [2–14,20–28]. The motion of the water in the penstock, its inertia and compressibility when it hits the turbine blades, and the elastic structure of the penstock naturally cause excessive water fluctuations. This phenomenon is called a water hammer. In large-scale power plants, surge tanks are used to prevent the damage to the mechanical components due to the excessive water fluctuations moving along the penstock. The incoming waves are absorbed in the surge tank. If the water velocity is in the range of 2.5–7 m/s, the surge tanks can be taken into account only in the hydraulic power plants with a long penstock.

The generator actuated by a hydraulic turbine can be represented by a large mass rotating under two opposite direction moment loads. When the mechanical moment T_m increases the rotation speed, the electrical moment T_e has a counter-effect to reduce the speed. When both moments are equal in magnitude, the rotation speed of the turbine becomes constant ($\omega = \omega_0$). If the electrical load is increased, i.e. T_e is greater than T_m, the whole system starts to decelerate. Since an excessive deceleration may harm the system, it is required to increase the mechanical moment. This process is made possible by setting a balance between the moments so that the turbine rotates with a required and acceptable speed. The generator equations to carry out this process numerically were obtained by considering the equivalent circuit given in Figure 4.

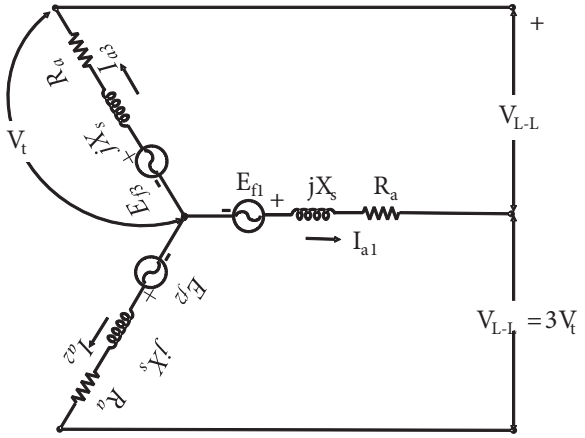

Figure 4. Equivalent circuit for a round rotor (cylindrical) synchronous generator [29].

The d-q reference frame transformation, also called the two-axis transformation, of the round rotor synchronous generator (equivalent circuit shown in Figure 4) will be used in the modeling [29]. The synchronous generator equations in the rotor reference frame are obtained as follows.

Voltage equations:

$$V_{qs} = R_s I_{qs} + \omega_r \lambda_{ds} + p\lambda_{qs} \tag{1}$$

$$V_{ds} = R_s I_{ds} - \omega_r \lambda_{qs} + p\lambda_{ds} \tag{2}$$

$$V_{fd} = R_{fd} I_{fd} + p\lambda_{qfd} \tag{3}$$

Flux linkage equations:

$$\lambda_{qs} = L_{ls} I_{qs} + L_m I_{qs} \tag{4}$$

$$\lambda_{qs} = L_{ls} I_{qs} + L_m.(I_{ds} + I_{fd}) \tag{5}$$

$$\lambda_{fd} = L_{lfd} I_{fd} + L_m.(I_{ds} + I_{fd}) \tag{6}$$

Equation of motion:

$$T_m = j\left(\frac{2}{p}\right) p\omega_r + T_e. + B\omega_r \tag{7}$$

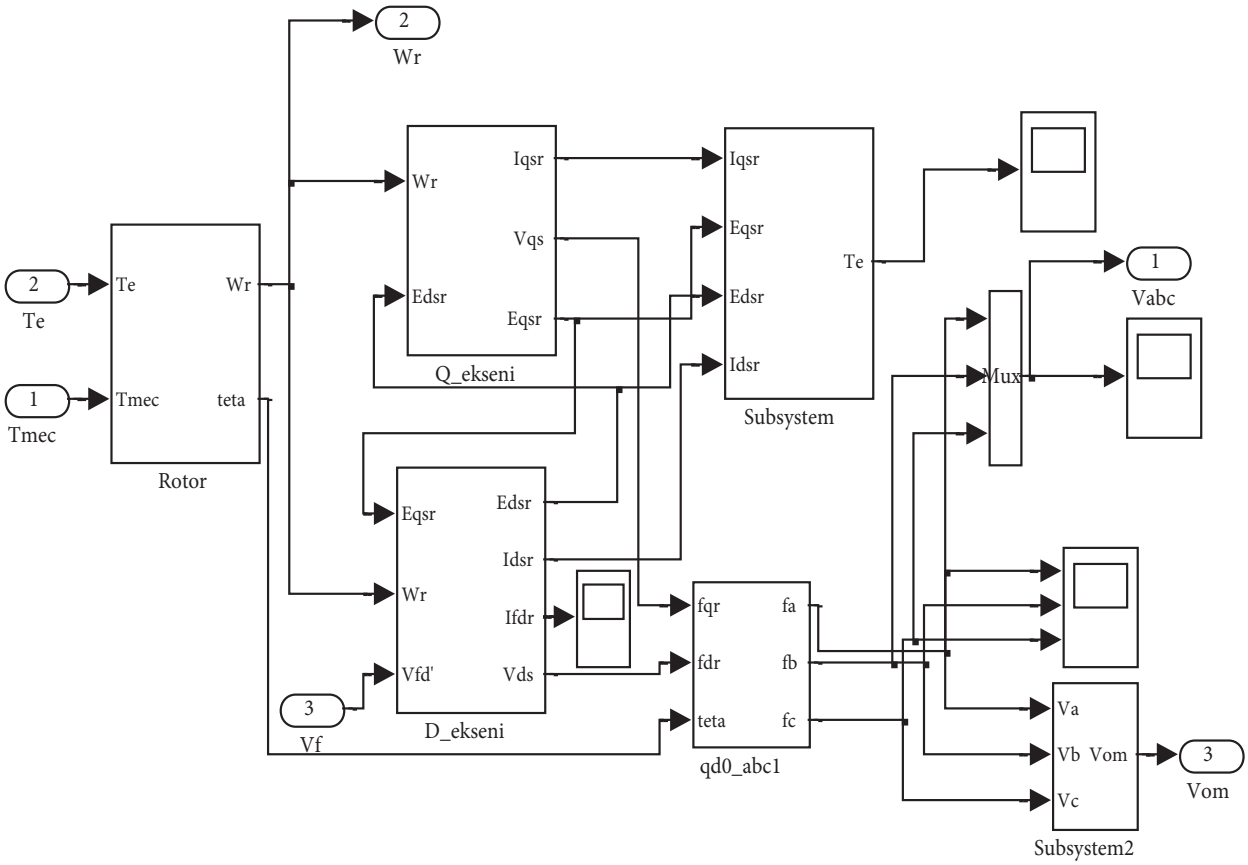

Figure 5. MATLAB/Simulink model of round rotor synchronous generator.

In these equations, the s subscript denotes the stator winding and the f subscript denotes the magnitude related to excitation winding. V, I, λ, R, T_e, and p denote voltage, current, flux linkage, resistance, moment, and number of poles, respectively. L_{ls} and L_{lfd} denote leakage inductance of stator winding and excitation winding, respectively. B is the friction coefficient. T_m and T_e are the mechanical and electrical moment loads, respectively. The MATLAB/Simulink model obtained from these equations is shown in Figure 5.

2.1. Nonlinear model of the microhydroelectric power plant

Fluid mechanics will be considered in the modeling of the part of the turbine from the water tank through the penstock up to the turbine, whereas the turbine mechanics will be considered in the modeling of the part that transforms the kinetic energy of the water into mechanical energy and turbine rotational speed. The hydraulic losses due to the friction inside the penstock are negligible in accordance with the system solution. Thus, they are not taken into account.

The following assumptions are made in the modeling:

- Hydraulic resistance (hydraulic losses) can be ignored.
- The penstock is rigid (not elastic) and the water is incompressible.
- The velocity of water is directly proportional to the square root of turbine needle aperture and net fall.
- Turbine mechanical power is directly proportional to the product of hydraulic fall and water velocity.

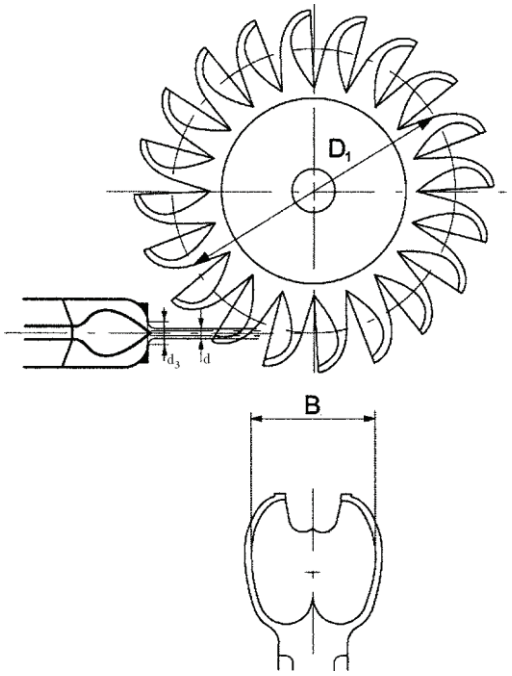

Figure 6. Pelton turbine and the turbine blade with its injector.

The power that can be extracted from water is given in Eq. (8). The efficiency of hydraulic turbines is as given in Eq. (9). The values indicated by subscripts 1 and 2 are the values at the first and last contact points of the water and the turbine, respectively. Figure 6 denotes the turbine structure and Figure 7 shows the velocity triangles.

$$P = Q\gamma g H_n.\eta_T \ (W) \tag{8}$$

$$\eta_h = \frac{U_1.C_1.cos\alpha_1 - U_2.C_2.cos\alpha_2}{g.H} \tag{9}$$

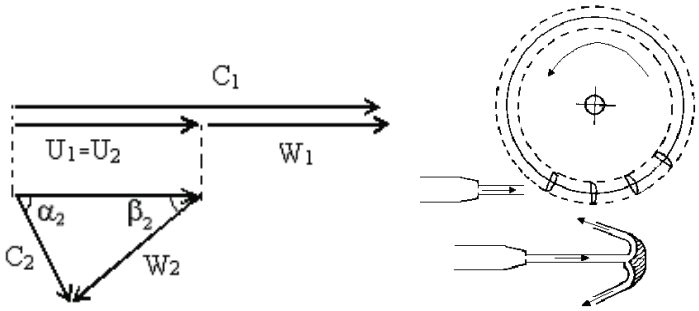

Figure 7. Inlet and outlet velocity triangle of the Pelton turbine.

The net fall is obtained as

$$H_n = k_v \frac{U}{g} (c_1 - U_c)(1 + \vartheta cos\beta) \tag{10}$$

considering the velocity triangles and treating the efficiency as a coefficient, whereby the M_d moment is obtained.

$$M_d = \frac{N}{\omega} \tag{11}$$

$$U_1 = \omega \frac{D}{2} \tag{12}$$

$$M_d = \mathrm{Q}.\gamma.k_v \frac{U}{\omega} \left(c_1 - \omega.\frac{D}{2} \right) (1 + \vartheta.cos\beta) \tag{13}$$

If the area where the water jet flows out is represented by S, the real flow rate (debit) can be written as follows.

$$Q = SC_1 \tag{14}$$

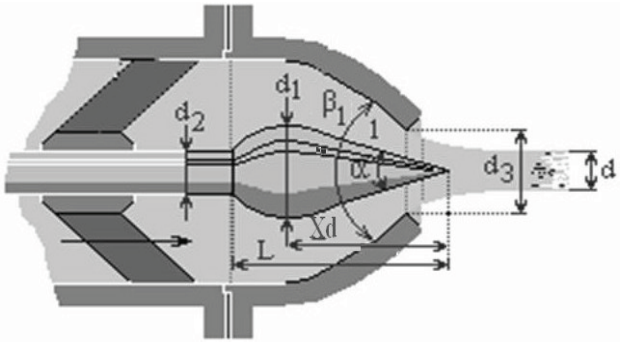

Figure 8. The injector and its parameters.

If the area S shown in Figure 8 is written as a function of X_d, Eq. (15) is obtained.

$$S = \pi[d^2 - (X_d \tan\frac{\alpha}{2})^2] \tag{15}$$

If Eq. (15) is substituted in Eq. (14), Eq. (16) is obtained.

$$\mathrm{Q} = \pi[d^2 - (X_d \tan\frac{\alpha}{2})^2]C_1 \tag{16}$$

$$C_1 = K_c\sqrt{2.g.H_{net}} \tag{17}$$

If Eq. (17) is substituted into Eq. (16),

$$\mathrm{Q} = \pi[d^2 - (X_d \tan\frac{\alpha}{2})^2]K_c\sqrt{2.g.H_{net}}. \tag{18}$$

In this way, all the necessary equations are obtained to build the nonlinear model of the Pelton turbine.

2.2. Purposed micro-Pelton turbine model

In the nonlinear model used for the numerical simulation of the Pelton turbine, the performance of the turbine under different conditions (the variable efficiency) should be taken into account to approach the real turbine behavior. There are several studies in the literature on the addition of turbine performance in the nonlinear model. The proposals in these studies do not provide complete solutions and require complex computational works [9,30–33]. In this study, the turbine efficiency curve is initially obtained as a simple and practical approach to increase the accuracy of the model. The efficiency equation is included in the nonlinear system with the help of this curve and a more realistic and simpler system is modeled without any complex calculation. This study is a pioneer application in Pelton turbines and MHPPs. A similar modeling approach was applied to a 34 MVA Kaplan turbine system by Brezovec et al. [34], but that study was out of the scope of MHPPs.

In the calculation of the turbine efficiency curve, the efficiency at different points is calculated and combined appropriately considering the general turbine characteristics. The efficiency curve obtained in this way is shown in Figure 9. Eq. (19) is obtained using this curve.

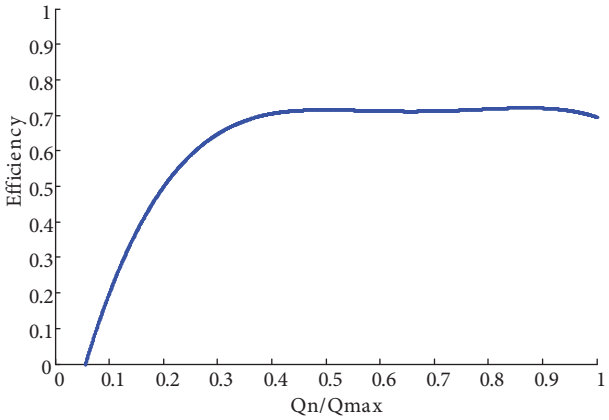

Figure 9. The efficiency curve of the Pelton turbine of the prototype MHPP.

$$\eta = -(1.4e-6) * Q_{pu}^4 + (8.1e-5) * Q_{pu}^3 - (1.6e-3) * Q_{pu}^2 + (1.5e-2) * Q_{pu} - 0.015 \tag{19}$$

The Q_{pu} value in Eq. (19) is the flow rate per unit (pu). Pressure setting is done to obtain the desired net fall in the prototype. It is seen that the manipulated pressure value changes in a certain band interval. A random function signal is added to the net fall to represent this change in the model. The model developed in MATLAB/Simulink is shown in Figure 10.

3. Results and discussion

To compare the numerical model obtained with the real turbine on the system, two different experiments were carried out. The experiments were done for different pressure values and needle apertures and as open-loop (without frequency control).

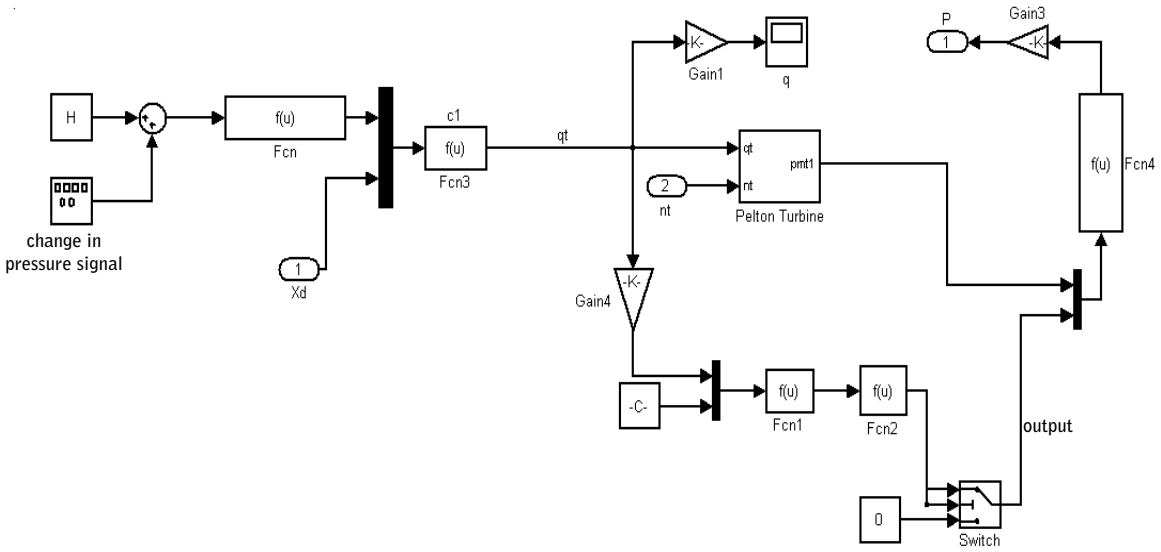

Figure 10. MATLAB/Simulink model of the Pelton turbine of the prototype MHPP.

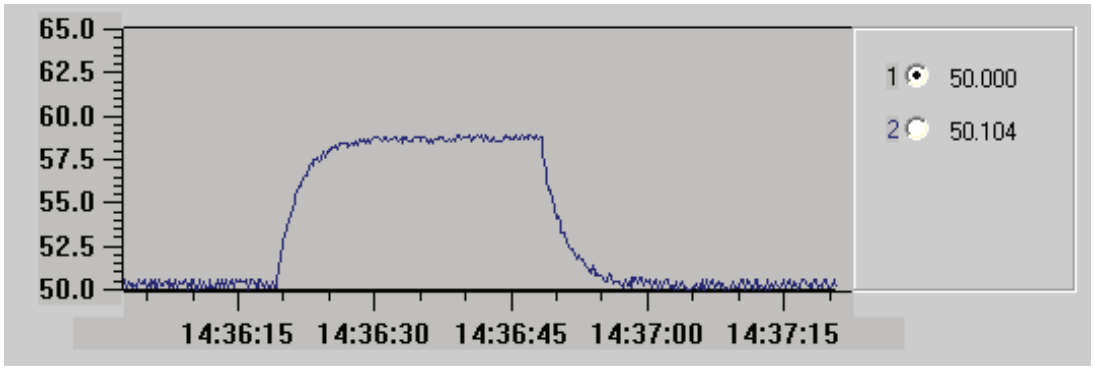

Figure 11. Load rejection experiment under 10 bar pressure (open-loop).

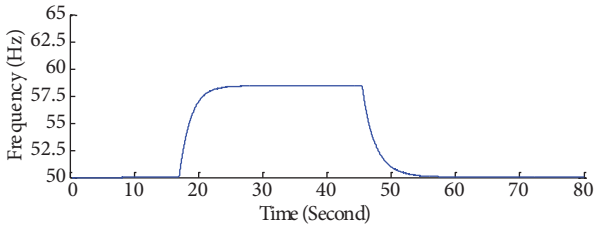

Figure 12. Load rejection simulation under 10 bar pressure (open-loop).

Figure 11 shows the experimental results of the transition of the open-loop prototype working under 10 bar pressure from 30% load condition to 15% load condition. Figure 12, on the other hand, shows the simulation results under the same conditions.

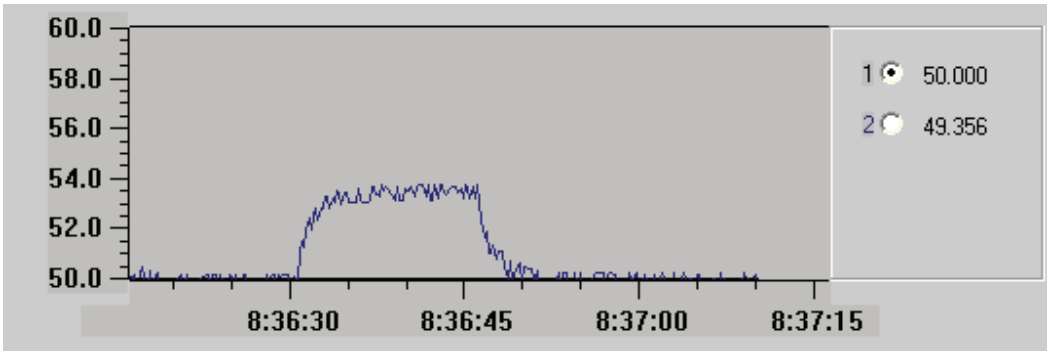

Figure 13. Load rejection experiment under 5 bar pressure (open-loop).

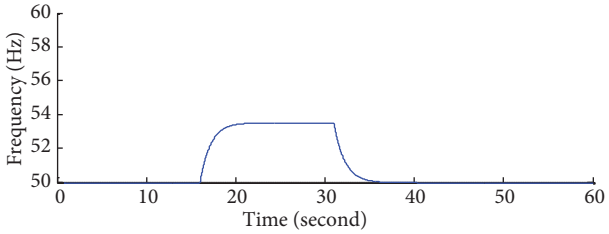

Figure 14. Load rejection simulation under 5 bar pressure (open-loop).

Figure 13 shows the experimental results of the transition of the open-loop prototype working under 5 bar pressure from 20% load condition to 10% load condition. Figure 14, on the other hand, shows the simulation results under the same conditions. The horizontal axis of the experimental results denotes the real time, whereas the vertical axis denotes the frequency (Hz). The results of the experiments are screenshots captured from a PLC S7 300 interface. Therefore, the experimental studies and the simulation studies could not be shown in the same platform. It is seen that the results obtained from the model and the real system, excluding the vibrations, are very close to each other, which proves the validity of the approach. The effects of very small variations in the pressure values on the speed were not observed in the simulations.

One of the disadvantages of the proposed method is that it cannot respond to very small and sudden changes, as is the case for all nonlinear turbine models. The developed model cannot respond to small changes in the pressure arising from the multistage pump providing the pressurized water in the system. The reason for that is the integral in the equation of motion. As is seen from the figures, the simulation results agree with the experimental results when there are considerable speed changes.

As the use of MHPPs enlarges, studies on them have been increasing. This study focused on a new approach that makes a nonlinear model of a Pelton turbine, which can be created by basic equations, more realistic. Thus, with the help of this approach, simulations studies to be performed will provide both less process time and more real-like results compared to other models. Therefore, the practical realizations of theoretical studies using the new approach will be easier.

4. Conclusion

In this study, a detailed nonlinear mathematical model of a MHPP with a Pelton turbine was developed and the results obtained from this model were compared to the experimental results obtained from the MHPP prototype in the laboratory.

The model developed by MATLAB/Simulink is a simpler and more realistic model compared to the complex models with adjusted parameters in the literature, and it is a reliable simulation tool for the tests and analyses of the system under stationary and changing operating conditions. With this model, the simulations of existing and developing control techniques can be carried out in a more realistic manner.

Acknowledgments

This study was produced from the PhD thesis of MT Özdemir (2012) conducted at the Graduate School of Natural and Applied Sciences of Fırat University and supported by FÜBAP (Project No: MF.11.06). The authors wish to thank Dr Abuzer Çalışkan for the measurement of the parameters of the prototype MHPP.

References

[1] World Energy Council, Turkish National Committee. Energy Report. Ankara, Turkey: DEK-TMK, 2010 (in Turkish).

[2] Fangtong X, Yonghua L, Qijuan C. Study of the modeling of hydroturbine generating set. In: International IEEE/IAS Conference on Industrial Automation and Control: Emerging Technologies; 22–27 May 1995; Taipei, Taiwan. New York, NY, USA: IEEE. pp. 644–647.

[3] Marinescu C, Clotea L, Cirstea M, Serban I, Ion C. Controlling variable load stand-alone hydro-generators. In: Proceedings of the Annual Conference of the IEEE Industrial Electronics Society; 6–10 November 2005; Raleigh, NC, USA. New York, NY, USA: IEEE. pp. 2554–2559.

[4] Salhi I, Doubabi S, Essounbouli N. Design and simulation of fuzzy controller and supervisor for a micro-hydro power plant. In: Control & Automation (MED), 2010 18th Mediterranean Conference; 23–25 June 2010; Marrakech, Morocco. New York, NY, USA: IEEE. pp. 1401–1406.

[5] Salhi I, Chennani M, Doubabi S, Ezziani N. Modeling and regulation of a micro hydroelectric power plant. In: IEEE International Symposium on Industrial Electronics; 30 June–2 July 2008; Cambridge, UK. New York, NY, USA: IEEE. pp. 1639–1644.

[6] Marquez JL, Molina MG, Pacas JM. Dynamic modeling, simulation and control design of an advanced micro-hydro power plant for distributed generation applications. Int J Hydrogen Energ 2010; 35: 5772–5777.

[7] Ion CP, Marinescu C. Control of parallel operating micro hydro power plants. In: Proceedings of the 12th International Conference on Optimization of Electrical and Electronic Equipment; 20–22 May 2010; Brasov, Romania. New York, NY, USA: IEEE. pp. 1204–1209.

[8] Marcelo GM, Pacas M. Improved power conditioning system of micro-hydro power plant for distributed generation applications. In: Industrial Technology (ICIT), 2010 IEEE International Conference; 14–17 March 2010; Valparaiso, Chile. New York, NY, USA: IEEE. pp. 1733–1738.

[9] Salhi I, Doubabi S, Essounbouli N, Hamzaoui A. Application of multi-model control with fuzzy switching to a micro hydro-electrical power plant. Renew Energ 2010; 35: 2071–2079.

[10] Scherer LG, Camargo RF, Pinheiro H, Rech C. Advances in the modeling and control of micro hydro power stations with induction generators. In: Energy Conversion Congress and Exposition (ECCE) 2011; 17–22 September 2011; Phoenix, AZ, USA. New York, NY, USA: IEEE. pp. 997–1004.

[11] Scherer LG, Camargo RF. Control of micro hydro power stations using nonlinear model of hydraulic turbine applied on microgrid systems. Brazilian Power Electronics Conference (COBEP); 11–15 September 2011; Natal, Brazil. New York, NY, USA: IEEE. pp. 812–818.

[12] Tischer CB, Posser C, Scherer LG, Franchi CM, Camargo RF. Hybrid method for control of voltage regulation applied in micro hydro power station. In: 38th Annual Conference of IEEE Industrial Electronics Society; 25–28 October 2012; Montreal Canada. New York, NY, USA: IEEE. pp. 1013–1018.

[13] Huang W, Yao K, Wu C, Wang S. Dynamic simulation and analysis of a low-voltage micro-grid. In: International Conference on Computing, Measurement, Control, and Sensor Network; 7–9 July 2012; Taiyuan, China. New York, NY, USA: IEEE. pp. 245–248.

[14] Özdemir MT. Active and reactive power control based on intelligent controller at micro hydro power plant. PhD, Fırat University, Elazığ, Turkey, 2012.

[15] UNIDO. Small Hydro Power Bulletin. New York, NY, USA: United Nations Industrial Development Organization Press, 1984.

[16] Jarman R, Bryce P. Experimental investigation and modelling of the interaction between an AVR and ballast load frequency controller in a stand-alone micro-hydroelectric system. Renew Energ 2007; 32: 1525–2543.

[17] Murthy SS, Singh B, Kulkarni A, Sivarajan R, Gupta S. Field experiences on a novel pico-hydel system using self-excited induction generator and electronic load controller. In: Proceedings of IEEE Fifth International Conference on Power Electronics and Drive Systems, Vol. 2; 17–20 November 2003; New York, NY, USA: IEEE. pp. 842–847.

[18] Öztürk D. Automatic control with PLC in the small hydroelectric power plant. MSc, Fırat University, Elazığ, Turkey, 2003.

[19] Dal M, Kaya AM, Aksit MF, Yigit SK, Kandemir I, Yuksel E. A hardware test setup for grid connected and island operation of micro hydro power generation systems. In: 2010 IEEE International Energy Conference and Exhibition; 18–21 December 2010; Manama, Bahrain. New York, NY, USA: IEEE. pp. 624–629.

[20] Hovey LM. Optimum adjustment of hydro governors on Manitoba hydro system. AIEE T 1962; 81: 581–558.

[21] Eke İ. Modelling and simulation of hydroelectric plants. MSc, Kırıkkale University, Kırıkkale, Turkey, 2004.

[22] Blair P, Wozniak L. Nonlinear simulation of hydraulic turbine governor system. Water Power and Dam Construction 1976: 23–26.

[23] Sanathanan CK. Accurate low order model for hydraulic turbine-penstock. IEEE T Energy Conver 1987; 2: 196–200.

[24] Sanathanan CK. A Frequency domain method for tuning hydro governors. IEEE T Energy Conver 1988; 3: 14–17.

[25] Vournas CD. Second order hydraulic turbine models for multimachine stability studies. IEEE T Energy Conver 1990; 5: 239–244.

[26] Vournas CD, Zaharakis A. Hydro turbine transfer functions with hydraulic coupling. IEEE T Energy Conver 1993; 8: 527–532.

[27] Hannett LN, Feltes JW, Fardanesh B, Crean W. Modeling and control tuning of a hydro station with units sharing a common penstock section. IEEE T Power Syst 1999; 14: 1407–1414.

[28] Kundur P. Power System Stability and Control. New York, NY, USA: McGraw-Hill, 1994.

[29] Krause PC. Analysis of Electric Machinery. London, UK: McGraw-Hill Books, 1986.

[30] Kishor N, Singh SP, Raghuvanshi AS. Dynamic simulations of hydro turbine and its state estimation based LQ control. Energ Convers Manage 2006; 47: 3119–3137.

[31] Li C, Zhou J. Parameters identification of hydraulic turbine governing system using improved gravitational search algorithm. Energ Convers Manage 2011; 52: 374–381.

[32] Bai J, Xie A, Yu X, Zhou L. Simulation model of hydraulic turbine speed control system and its parameters identification based on resilient adaptive particle swarm optimization algorithm. In: Asia-Pacific Power and Energy Engineering Conference; 28–31 March 2010; Chengdu, China. New York, NY, USA: IEEE. pp. 1–4.

[33] Trudnowski D, Agee J. Identifying a hydraulic-turbine model from measured field data. IEEE T Energy Convers 1995; 10: 768–772.

[34] Brezovec M, Kuzle I, Tomisa T. Nonlinear digital simulation model of hydroelectric power unit with Kaplan turbine. IEEE T Energy Convers 2006; 21: 235–241.